Inorganic Chemistry
Communication

Inorg. Chem. **2009**, *48*, 10883–10885 **10883**
DOI: 10.1021/ic9016454

(I,0) Mixed-Valence State of a Diiron Complex with Pertinence to the [FeFe]-Hydrogenase Active Site: An IR, EPR, and Computational Study

Pradyumna S. Singh,[†,⊥] Hans Christian Rudbeck,[†,#] Ping Huang,[†] Salah Ezzaher,[†] Lars Eriksson,[§] Matthias Stein,[*,‡] Sascha Ott,[*,†] and Reiner Lomoth[*,†]

[†]*Department of Photochemistry and Molecular Science, The Ångström Laboratories, Uppsala University, BOX 532, 751 20 Uppsala, Sweden,* [‡]*EML Research gGmbH, Molecular and Cellular Modeling, Schloss-Wolfsbrunnenweg 33, 69118 Heidelberg, Germany, and* [§]*Department of Physical, Inorganic and Structural Chemistry, Stockholm University, 106 91 Stockholm, Sweden.* [⊥]*Present address: Kavli Institute of Nanoscience, Delft University of Technology, Lorentzweg 1, 2628 CJ Delft, The Netherlands.* [#]*Present address: Danish Power Systems ApS, Raadhusvej 59, 2920 Charlottenlund, Denmark.*

Received August 17, 2009

Biphenyl-2,2′-dithiolate (bpdt) bridged $Fe_2(bpdt)(CO)_6$ (**1**) undergoes two sequential electrochemically quasi-reversible reductions. The one-electron reduction product $\mathbf{1}^-$ is unusually stable against irreversible structural changes and could be characterized by IR and EPR spectroscopy supported by computational methods. Reduction to the (I,0) state does not trigger bridging coordination of CO but partial deligation of the dithiolate in $\mathbf{1}^-$ that ultimately forms a diamagnetic dimerization product.

The design of molecular catalysts for the reduction of protons to dihydrogen is a key aspect of the overall challenge of artificial photosynthesis.[1,2] Inspiration for such molecular catalysts has been taken from the active site structure of the [FeFe] hydrogenase enzymes[3,4] that are efficient catalysts for this reaction.[5] Much effort has been directed toward the synthetic modeling of their active site, and the principal ability of the hydrogenase mimics to generate hydrogen from protons at reduced overpotential has been frequently demonstrated in electrocatalytic experiments.[6−9] More recently, hydrogenase mimics have also been successfully employed as catalysts in photochemical hydrogen production.[10−12]

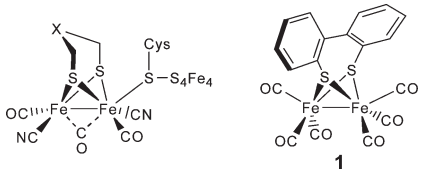

1

Insight into the catalytic cycle is, however, rather limited with respect to the identification of catalytic intermediates, and their spectroscopic characterization in oxidation states below the initial $[Fe^I-Fe^I]$ level has remained a major challenge. The observation of reduced intermediates[13] is usually impeded by rapid catalytic turnover in the presence of protons, and by limited stability (CO loss, dimerization)[14−16] in absence of the substrate. If the usual aliphatic dithiolate bridging ligands are replaced with benzene-1,2-dithiolate (bdt), stable reduction products are obtained that only feature reversible intramolecular rearrangements. In contrast to their aliphatic counterparts, the bdt complexes[17−19] are,

*To whom correspondence should be addressed. E-mail: matthias.stein@eml-r.villa-bosch.de (M.S.); Sascha.Ott@fotomol.uu.se (S.O.); Reiner.Lomoth@fotomol.uu.se (R.L.).

(1) Lewis, N. S.; Nocera, D. G. *Proc. Natl. Acad. Sci. U.S.A.* **2006**, *103* (43), 15729–15735.
(2) Lubitz, W.; Reijerse, E. J.; Messinger, J. *Energy Environ. Sci.* **2008**, *1* (1), 15–31.
(3) Peters, J. W.; Lanzilotta, W. N.; Lemon, B. J.; Seefeldt, L. C. *Science* **1998**, *282*(5395), 1853–1858.
(4) Nicolet, Y.; Piras, C.; Legrand, P.; Hatchikian, C. E.; Fontecilla-Camps, J. C. *Structure* **1999**, *7*(1), 13–23.
(5) Adams, M. W. *Biochim. Biophys. Acta* **1990**, *1020*(2), 115–45.
(6) Capon, J.-F.; Gloaguen, F.; Pétillon, F. Y.; Schollhammer, P.; Talarmin, J. *Coord. Chem. Rev.* **2009**, *253*(9−10), 1476–1494.
(7) Tard, C.; Pickett, C. J. *Chem. Rev.* **2009**, *109*(6), 2245–2274.
(8) Gloaguen, F.; Rauchfuss, T. B. *Chem. Soc. Rev.* **2009**, *38*(1), 100–108.
(9) Felton, G. A. N.; Mebi, C. A.; Petro, B. J.; Vannucci, A. K.; Evans, D. H.; Glass, R. S.; Lichtenberger, D. L. *J. Organomet. Chem.* **2009**, *694*(17), 2681–2699.
(10) Na, Y.; Wang, M.; Pan, J.; Zhang, P.; Akermark, B.; Sun, L. *Inorg. Chem.* **2008**, *47*(7), 2805–2810.
(11) Streich, D.; Astuti, Y.; Schwartz, L.; Lomoth, R.; Hammarström, L.; Ott, S *Chem.—Eur. J.* **2009**, accepted.
(12) Kluwer, A. M.; Kapre, R.; Hartl, F.; Lutz, M.; Spek, A. L.; Brouwer, A. M.; van Leeuwen, P.; Reek, J. N. H. *Proc. Natl. Acad. Sci. U.S.A.* **2009**, *106*(26), 10460–10465.
(13) Chong, D.; Georgakaki, I. P.; Mejia-Rodriguez, R.; Sanabria-Chinchilla, J.; Soriaga, M. P.; Darensbourg, M. Y. *Dalton Trans.* **2003**, *21*, 4158–4163.
(14) Borg, S. J.; Behrsing, T.; Best, S. P.; Razavet, M.; Liu, X.; Pickett, C. J. *J. Am. Chem. Soc.* **2004**, *126*(51), 16988–16999.
(15) Borg, S. J.; Tye, J. W.; Hall, M. B.; Best, S. P. *Inorg. Chem.* **2007**, *46* (2), 384–394.
(16) Aguirre de Carcer, I.; Di Pasquale, A.; Rheingold, A. L.; Heinekey, D. M. *Inorg. Chem.* **2006**, *45*(20), 8000–8002.
(17) Capon, J. F.; Gloaguen, F.; Schollhammer, P.; Talarmin, J. *J. Electroanal. Chem.* **2004**, *566*(2), 241–247.

Published on Web 11/04/2009

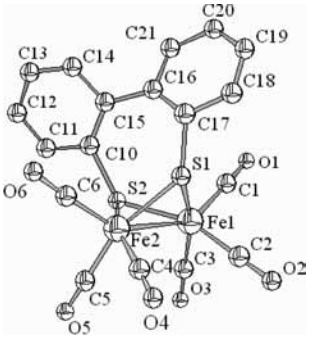

Figure 1. Thermal ellipsoid plot of the solid-state structure of $Fe_2(\mu$-bpdt$)(CO)_6$ at the 50% probability level (hydrogen atoms omitted for clarity). Bond distance Fe(1)−Fe(2), 2.534 Å; torsion angle between the phenyl rings C(10)−C(15)−C(16)−C(17), 51.24°.

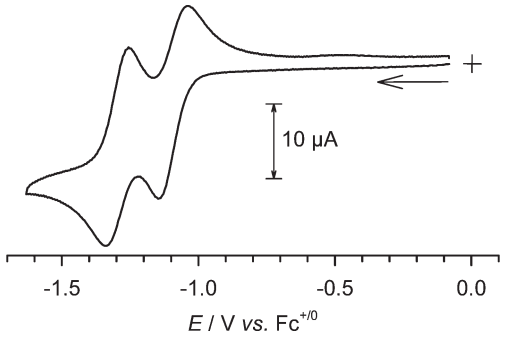

Figure 2. Cyclic voltammogram (0.100 V s^{-1}) of **1** (1 mM) in CH_3CN with 0.1 M $[N(n\text{-}C_4H_9)_4]^+[PF_6]^-$.

however, reduced in a two-electron process, which precludes the observation of the $[Fe^I-Fe^0]$ state.[20]

Here we report on the first example of a diiron hexacarbonyl complex with a biphenyl-2,2′-dithiolate (bpdt) bridging ligand, Fe_2(bpdt)$(CO)_6$ (**1**). **1** was prepared in 41% yield from bpdt and $Fe_3(CO)_{12}$ in refluxing THF, and its structure confirmed by X-ray crystallography (Figure 1). The torsion angle of 51° between the two phenyl rings reduces their conjugation, which results in CO vibrational frequencies that are largely identical to those of Fe_2(bdt$)(CO)_6$.[18]

Voltammograms of **1** in acetonitrile solution (Figure 2) show two electrochemically quasi-reversible one-electron waves at $E_{1/2} = -1.09$ V ($\Delta E_p = 112$ mV at 0.1 V s^{-1}) and −1.30 V vs $Fc^{+/0}$ ($\Delta E_p = 92$ mV) that can be attributed to the $[Fe^I-Fe^I]/[Fe^I-Fe^0]$ and the $[Fe^I-Fe^0]/[Fe^0-Fe^0]$ couples, respectively. From the chemical reversibility and separation of the voltammetric waves with the resulting low disproportionation constant ($K_{dis} = \exp(-\Delta E_{1/2}F/RT) = 2.84 \times 10^{-4}$, $\Delta G°_{dis} = 20.3$ kJ mol^{-1}), it was anticipated that one-electron reduction of **1** offers a possibility to obtain spectroscopic signatures of the $[Fe^I-Fe^0]$ state.

Figure 3 shows the IR absorption changes in the carbonyl region that were induced by reduction at −1.23 V vs. $Fc^{+/0}$. The consumption of **1** is followed by the bleaching of its three carbonyl bands at 2079, 2045, and 2005 cm^{-1} (cf. Figure 4a).

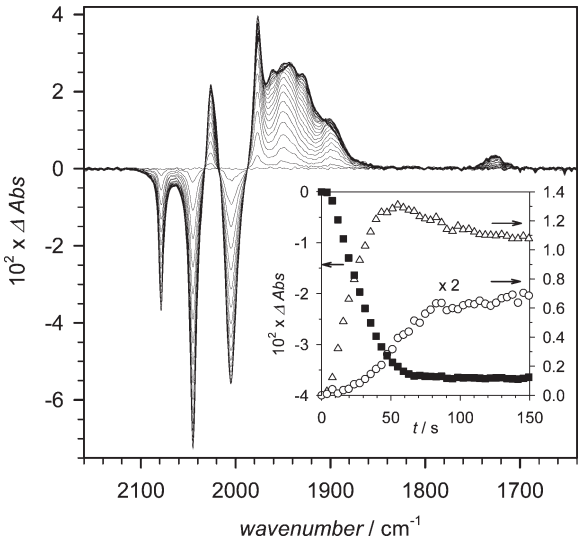

Figure 3. IR spectroelectrochemical changes induced by reduction of **1** (1.5 mM) at −1.23 V vs $Fc^{+/0}$ in CH_3CN with 0.1 M $[N(n\text{-}C_4H_9)_4]^+$-$[PF_6]^-$. Inset: Absorbance vs time traces for 2079 cm^{-1} (■), 1899 cm^{-1} (Δ), and 1725 cm^{-1} (○).

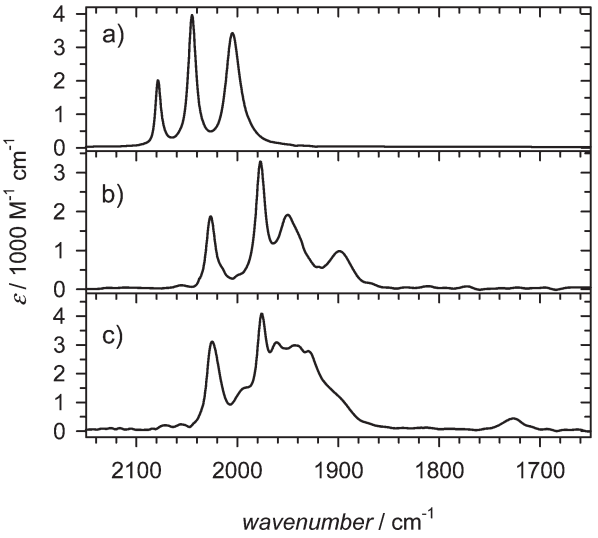

Figure 4. IR spectra of (a) **1**, (b) the primary reduction product $\mathbf{1}^-$, and (c) the final product $[\mathbf{1}_2]^{2-}$ in CH_3CN with 0.1 M $[N(n\text{-}C_4H_9)_4]^+$ $[PF_6]^-$.

The product absorption is initially characterized by four well-resolved absorption bands (2026, 1977, 1950, 1899 cm^{-1}) that subsequently evolve into a more complex spectrum. The kinetics of this transformation (Inset Figure 3) is strongly convoluted with the rate of electrolysis. The IR spectrum of the primary product (Figure 4b) could however be obtained from the absorption changes acquired during early stages of electrolysis (16 s) that were scaled according to the corresponding consumption of **1**. The appearance of additional bands rather than a simple shift toward lower wavenumbers upon reduction is indicative of some structural rearrangement already in the primary reduction product, which could be elucidated from computational studies (see below). From the absence of IR bands below 1800 cm^{-1}, it is evident, however, that no structure with bridging carbonyl ligand(s) is formed initially. This is in contrast to complexes with aliphatic dithiolate ligands that rapidly form μ-CO species upon reduction.[14] Decoordination of thiolate ligands is an

(18) Felton, G. A. N.; Vannucci, A. K.; Chen, J.; Lockett, L. T.; Okumura, N.; Petro, B. J.; Zakai, U. I.; Evans, D. H.; Glass, R. S.; Lichtenberger, D. L. *J. Am. Chem. Soc.* **2007**, *129*(41), 12521–12530.
(19) Capon, J. F.; Gloaguen, F.; Schollhammer, P.; Talarmin, J. *J. Electroanal. Chem.* **2006**, *595*(1), 47–52.
(20) Felton, G. A. N.; Petro, B. J.; Glass, R. S.; Lichtenberger, D. L.; Evans, D. H. *J. Am. Chem. Soc.* **2009**, *131*, 11290–11291.

Chart 1. Reduction Products of **1** (See the Supporting Information for DFT Optimized Structures)[a]

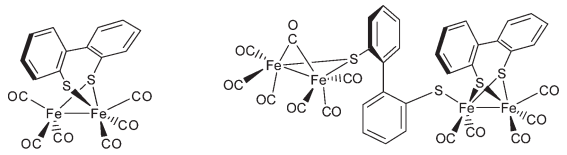

1$^-$ $[\mathbf{1_2}]^{2-}$

[a] Computed Fe−Fe bond distances: 2.55 Å (**1**), 2.56 Å (**1**$^-$), 2.57 Å ($[\mathbf{1_2}]^{2-}$, $Fe_2(CO)_7$), and 2.55 Å ($[\mathbf{1_2}]^{2-}$, $Fe_2(CO)_5$).

alternative response to reduction, and with aliphatic dithiolates detachment of one thiolate group from both Fe centers is known to occur after two-electron reduction.[14] In case of **1**, superior agreement between the experimental and computational IR spectra (see the Supporting Information) of the one-electron reduced complex was obtained for a structure with one broken Fe−S bond (**1**$^-$, Chart 1) rather than an alternative μ_2:μ_2 Fe^0Fe^I species. Compared to the latter structure, **1**$^-$ is more stable by 8 kcal/mol (B3LYP/TZVP results) while geometry optimizations starting from a μ_1:μ_1 [Fe^0Fe^I] with two broken Fe−S bonds converged back to the μ_1:μ_2 [Fe^0Fe^I] structure.

The final product (Figure 4c) is distinguished from **1**$^-$ by less-resolved bands in the terminal CO region (2025, 1976, 1961, 1943, 1930 cm^{-1}), and most notably by a μ-CO band at 1727 cm^{-1} (Figure 4c). These features can be attributed to a dimeric structure where a dithiolate links two diiron units with five and seven CO, respectively ($[\mathbf{1_2}]^{2-}$, Chart 1). The assignment is based on the detailed agreement of the IR spectrum with the reported spectrum of a crystallographically characterized dimer derived from the propyldithiolate analogue.[16] In the pdt analogue, the dimer was formed by reaction between the two-electron reduction product and the parent complex.[14] Formation of $[\mathbf{1_2}]^{2-}$ under the conditions of spectroelectrochemical experiments might follow the same mechanism as dimerization might drive the disproportionation equilibrium.

While **1** is EPR silent as expected for an antiferromagnetically coupled [Fe^I−Fe^I] species, controlled potential electrolysis at −1.19 V resulted in a paramagnetic product with an EPR spectrum shown in Figure 5. The same rhombic product spectrum (g = 2.060, 2.048, 2.003) of an S = 1/2 species was obtained by reduction with one equivalent of cobaltocene (−1.329 V vs $Fc^{+/0}$ in acetonitrile),[21] and with the samples annealed to room temperature the EPR signals decayed on the same time scale as the IR spectrum assigned to **1**$^-$. Further evidence for the assignment of the EPR signal to **1**$^-$ was provided by comparison to computational results (g = 2.049, 2.033, 2.003, inset Figure 5 and Supp. Inf.) obtained for **1**$^-$ with one broken Fe−S bond. The unpaired electron spin in **1**$^-$ localizes almost exclusively on the five-coordinate atom (ρ(Fe) = 1.22) for which a +1 oxidation state can be assigned. The six-coordinate Fe^0 atom only carries a minor part of unpaired spin due to spin-polarization (ρ(Fe) = −0.26). Broken-symmetry calculations collapsed back to the spin-localized state. The decay of **1**$^-$ does not give rise to any paramagnetic species and the

(21) Shalev, H.; Evans, D. H. *J. Am. Chem. Soc.* **1989**, *111*(7), 2667–74.

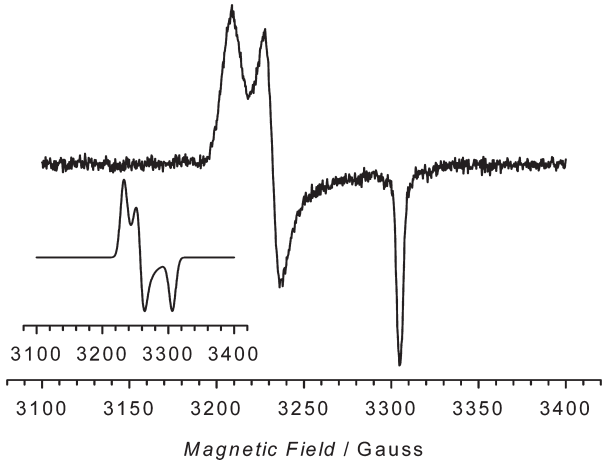

Figure 5. X-band EPR spectra of **1**$^-$ (at 9.5 K) obtained by electrochemical reduction of **1** (1 mM in CH_3CN) at −1.19 V vs. $Fc^{+/0}$ (after 25 s of electrolysis). Inset simulated spectrum with the DFT optimized structure of **1**$^-$ according to Chart 1. EPR parameters: microwave frequency, 9.27 GHz; modulation frequency, 100 kHz; modulation amplitude, 0.5 G; microwave power, 0.2 μW.

electronic structure of the dimerization product has to be described as [Fe^I−Fe^I]−[Fe^0−Fe^0] rather than [Fe^I−Fe^0]$_2$, in accordance with the distinguished ligand sets of the two subunits in $[\mathbf{1_2}]^{2-}$.

In summary, it could be shown that the biphenyldithiolate bridging ligand brings about an unprecedented reactivity of the reduced diiron hexacarbonyl complex. Compared to aliphatic counterparts, a relatively stable one-electron reduction product **1**$^-$ is formed with no indications for loss of CO or formation of μ-CO. Reversible changes of the thiolate coordination, presumably a μ_2 to μ_1 rearrangement, appear to be the only response to one-electron reduction, whereas the slow dimerization process that limits the lifetime of **1**$^-$ presumably involves disproportionation. As a result of the structural changes on the one-electron reduction level, the half-wave potentials for first and second reduction of **1** are close but normally ordered. This is in contrast to the bdt analogue that undergoes a two-electron reduction[18] with potential inversion.[22]

The IR- and EPR-spectroscopic signatures established in this study should be directly relevant to the recognition of reduced intermediates in the catalytic cycles of **1** and related compounds in electrochemical and light-driven hydrogen formation schemes.

Acknowledgment. Financial support from the Swedish Research Council (VR), the Swedish Energy Agency, the Knut and Alice Wallenberg Foundation, the Klaus Tschira Foundation, and the EU (FP7 Energy 212508 "SOLAR-H2") is gratefully acknowledged.

Supporting Information Available: Experimental details and computational IR and EPR data for alternative structures of the reduced complex (PDF). Crystallographic information file. This material is available free of charge via the Internet at http://pubs.acs.org.

(22) Potential inversion refers to the situation where the uptake of the second electron occurs at a potential less negative than that for the uptake of the first electron.